Wetting Transition in a Molten Metal and Solid Substrate System in High Magnetic Fields

YUBAO XIAO, TIE LIU, ZHENGYANG LU, GUOJIAN LI, SHUANG YUAN, NORIYUKI HIROTA, ZHONGMING REN, and QIANG WANG

Wetting transitions between molten metals and different solid substrates were investigated using the sessile drop method to evaluate the possibilities of regulating wettability by high magnetic fields (HMFs) during wetting. For most wetting counterparts, the molten-metal droplet outline showed an apparent change because of the influence of HMFs. Contact angles that were measured with HMFs decreased compared with contact angles that were measured without HMFs. The temperature and magnetic-flux density had an evident but more complicated effect on the wetting transition. For reactive wetting systems, the effect of HMFs on changes of element distributions at the metal/substrate interface may lead to a variety of wetting transitions. For non-reactive wetting systems, solidified metal droplets can move from the solid substrates after wetting. No detailed and comprehensive explanations on HMF wetting-transition mechanisms exist, and further work is required. This study contributes to perfect wetting mechanisms and theories and provides a scientific approach to control wettability.

https://doi.org/10.1007/s11661-020-05706-3

I. INTRODUCTION

A water droplet can roll freely in a spherical shape on a lotus leaf; however, it spreads to flatness on glass. This phenomenon indicates diverse wetting transitions in nature. The contact angle, which is the most-used wetting-transition characteristic parameter, can reflect different wetting transitions between liquid droplets and solid substrates. In general, contact angles that change from 0 to 90 deg indicate a wetting status, whereas, a contact angle from 90 to 180 deg reveals a non-wetting status. The pursuit of a better wetting status, namely a smaller contact angle, is of importance in many fields, such as in metal-matrix composite manufacturing,[1] soldering,[2] electronic packaging,[3] and coating,[4] to regulate material performance.

The wetting transition of molten metal that is in contact with a solid substrate has been the subject of intensive wettability investigations for over 100 years. The formation of a reaction layer at the solid-liquid interface allows for a classification of non-reactive and reactive wetting. For non-reactive wetting, changes in surface energy,[5] viscosity,[6] and substrate roughness[7] lead to different wetting transitions. For reactive wetting, the temperature,[8] wetting atmosphere,[9] and material composition[10] affect the flowing status in liquid droplets,[11] solid-liquid interface behaviors,[12] and the reaction extent[13] to trigger a variation in wetting transition. Because of the effect of many factors, there is no comprehensive understanding of the wetting-transition mechanisms. Furthermore, wetting-transition theory is varied because of a wide variety of different material attributes that induce distinct wetting transitions. Further probing of the wetting transition of molten metals on solid substrates can provide insight into understand wetting transitions.

Based on previous research, endeavors aimed at improving wettability have focused primarily on changing the wetting-effect factors. An increase in temperature,[14] improvement in vacuum degree,[15] and modification in substrate configuration[16] are effective ways to decrease the contact angle. However, the difficulty of designing the experimental apparatus limits the further change of these factors. For instance, a

YUBAO XIAO is with the Key Laboratory of Electromagnetic Processing of Materials (Ministry of Education), Northeastern University, No. 11, Lane 3, WenHua Road, HePing District, Shenyang, 110819 Liaoning, P.R. China and also with the School of Materials Science and Engineering, Northeastern University, Shenyang 110819, P.R. China. TIE LIU, GUOJIAN LI, and QIANG WANG are with the Key Laboratory of Electromagnetic Processing of Materials (Ministry of Education), Northeastern University. Contact e-mail: liutie@epm.neu.edu.cn ZHENGYANG LU is with the Key Laboratory of Electromagnetic Processing of Materials (Ministry of Education), Northeastern University and also with the School of Metallurgy, Northeastern University, Shenyang 110819, P.R. China. SHUANG YUAN is with the School of Metallurgy, Northeastern University. NORIYUKI HIROTA is with the Fine Particle Engineering Group, National Institute for Materials Science, 3-13 Sakura, Tsukuba, Japan. ZHONGMING REN is with the State Key Laboratory of Advanced Special Steel, Shanghai University, Shanghai 200072, China.

Manuscript submitted October 9, 2019.
Article published online March 13, 2020

higher temperature favors a better wetting transition, but may challenge the design and manufacture of a suitable wetting device. The increase in temperature may lead to molten-metal evaporation, which is not an intrinsic wetting transition during wetting.[17] A new way to modify the wetting transition of molten metal on a solid substrate would be useful for realistic usage requirements and the simultaneous improvement in wetting status.

The application of a high magnetic field (HMF) in material processing provides options for new scientific research.[18] Because of a stronger Lorentz force, magnetic force, magnetic energy, and enhanced orientation function, HMF influences the melt flow,[19] energy transmission,[20] microstructure formation,[21] and interface behavior.[22] Extensive research has been conducted on HMFs, and many significant and influential discoveries have been made.[23–25] The merit of HMF impact on physical processes in a contactless way makes the development and design that contributes to conducting explorative research on HMFs flexible. Therefore, HMFs have also been introduced in wetting-transition research. In HMF, the contact angle between water droplets and the solid surface has been measured, and the results show that the contact angle tended to be larger than that measured without a magnetic field.[26] The wetting transition of water on a polymethyl methacrylate surface was better because the contact angle decreased under the influence of HMF compared with the contact angle measured without HMF.[27]

The reported studies show that different research results and opinions exist on HMF wetting-transition research and no consensus exists on the wetting-transition mechanism to explain the function of HMF during wetting. Limited previous work has explored the wetting transition of room-temperature liquid on solid surfaces, and few efforts have been concentrated on the wetting transition of molten metal on solid substrates in HMFs. An understanding of the wetting-transition mechanism of molten metal on a solid substrate in HMFs would help to improve the solidification technology, develop a new composite material, and promote the development of related fields.

Because of the current status, wetting transitions of different solid substrates that had been wetted by molten metals in HMFs were studied by the sessile drop method in the present study. Equipment for use in HMF was developed to conduct wetting experiments.[28] To investigate the influence of HMF on different magnetic materials during wetting, paramagnetic molten Al[29] and diamagnetic molten Sn[30] were selected as raw droplet materials. Some commonly used substrates that react with molten Al, *i.e.*, AlN[31] and SiO_2,[32] and those that do not react with molten Sn (*i.e.*, SiC,[33] C,[34] and Mo[35]) were selected. Sample photographs were recorded during wetting, and the wetting status is reflected by contact angles that were measured from these photographs. The contact angles between molten metals and different solid substrates in different HMFs at various temperatures were measured. The contact angles decreased when an external HMF was applied, and the wetting behavior was improved with the HMFs. Such decreases were strongly dependent on wetting conditions, in other words, the temperature, magnetic-flux density, and substrate pattern. Some detailed feasible mechanisms are discussed for the different wetting counterparts.

II. EXPERIMENTAL

A. *Materials*

High-purity metals were used in the experiment (99.999 wt pct). Al and Sn samples were 3 mm in diameter and 3 mm in height. Solid substrates were aluminum nitride (AlN), silica (SiO_2), silicon carbide (SiC), graphite (C), and molybdenum (Mo), and these substrates were 20 mm long, 20 mm wide, and 3 mm thick. One side of the substrate was polished to the conventional experimental-standard roughness, and the roughness was measured by an atomic force microscope (AFM). Five measurements were performed for each substrate with a scanning area of 10 μm × 10 μm, and these values were averaged to obtain a statistically significant result. The detailed material information is listed in Table I. The raw materials were preserved in a vacuum drying oven before the wetting experiments to prevent sample contamination. Pure Al, Sn, and the substrate were cleaned ultrasonically three times in acetone before every wetting experiment.

B. *Experimental Facility*

The experimental wetting-transition research facility in which the HMFs were used has been detailed in a previous work.[28] Pure metal and substrate were placed in the center of the superconducting magnet, and the metal/substrate interface was perpendicular to the gravity direction and parallel to the magnetic field direction. Solid pure metal can be heated to a molten state in a furnace. The superconducting magnet can regulate its magnetic-flux density from 0 to 6 T. The light source guarantees an optimal observation background so that high-quality images can be captured and reserved by observation and the image-manipulation system. The sample images that were recorded in the wetting process made it possible to obtain contact angles of molten metals on solid substrates measured by using the JGW-360 software with a measuring accuracy of 0.01 deg based on the Laplace-Young equation. A high vacuum level from 10^{-3} to 10^{-5} Pa was achievable. The wetting temperature was monitored by two S-type thermocouples close to the substrate base and furnace wall, respectively.

C. *Experimental Procedure*

A typical contact angle measuring process without magnetic field was performed in the following way. A sample was adjusted to a horizontal position by using a spirit level. The furnace chamber was enclosed and evacuated to 4×10^{-4} Pa. Pure metal was heated at 15 °C/min to the desired temperature. The wetting

Table I. Physical Characteristic Parameters of Raw Materials

Item	Al	Sn	AlN	SiO_2	SiC	C	Mo
Purity (Wt Pct)	99.999	99.999	99.9	99.99	99.5	99.99	99.95
Roughness (Ra/nm)	—	—	26	< 1	5	9	7
Dimension (mm^3)	Φ3 × 3	Φ3 × 3	Φ20 × 3	Φ20 × 3	Φ20 × 3	Φ20 × 3	Φ20 × 3

Table II. Applied Wetting Temperatures (°C) and Magnetic-Flux Density (T)

Magnetic-Flux Density (T)	0			2			4			6		
Temperature (°C) (for Al)	690	720	750	690	720	750	690	720	750	690	720	750
Temperature (°C) (for Sn)	278	300		278	300		278	300		278	300	

temperatures selected for the Al were 690 °C, 720 °C, and 750 °C, and for Sn, they were 278 °C and 300 °C, respectively. An isothermal period of 20 min was maintained after the experimental temperature was reached, and the sample images were photographed and recorded. After the isothermal period, the furnace stopped working and was cooled naturally. The sample was removed from the furnace as the experimental temperature decreased to room temperature. For the experiments in high magnetic fields, the measuring process is similar to that done without a magnetic field. The high magnetic field was increased to the desired magnetic flux density before heating the samples and decreased to zero when the temperature was lower than the melting point of pure metals. The magnetic flux densities were 0, 2, 4, and 6 T (Table II). For the experiments under different conditions, different pure metal specimens and substrates were used. Selected experiments were repeated two times under the same conditions with different specimens to confirm the high magnetic field effects. In total, except for the repeated experiments, 48 pure metal samples and 48 substrates were used in this work.

After the wetting experiments, some samples were sectioned vertically to prepare metallographic specimens. Macrosample photos were made using a digital camera (DSC-TX10, Sony). Microstructures of the measured samples were observed by scanning electron microscope (SEM, ULTRA PLUS), and the alloying element distributions near the interface between the molten metal and the substrate were identified by energy-dispersive spectrum (EDS) analysis.

III. RESULTS

A. *Morphologies of Molten Al and Sn Droplets During Wetting*

Pictures that were recorded during the wetting process reflect the wetting status of molten metal that spreads on a solid substrate. The morphologies of Al/AlN and Al/SiO_2 samples during wetting are shown in Figures 1(a) through (d). For Al/AlN, the shape of the molten Al was approximately spherical without a magnetic field. At a 6 T HMF, the molten Al outline became ellipsoidal. Without HMF, an ellipsoid molten Al droplet formed on the SiO_2 substrate surface. With application of a 6 T HMF, the profile of molten Al became hemispherical. These results indicate that the wetting behaviors of the Al/AlN and Al/SiO_2 counterparts are regulated largely by the HMF.

Figures 1(e) through (j) presents lateral views of different substrates that had been wetted by molten Sn at 300 °C. For Sn/SiC, an evident profile transformation occurred, and the shape of the molten Sn drop changed from ellipsoidal at 0 T to hemispherical at 6 T. The variation was similar for the Sn/C and Sn/Mo counterparts. Without HMF, the geometrical forms of molten Sn were hemispherical, and spreading hemispherical drops were visible for 6 T HMF. Distinct spreading statuses and outlines of molten Sn droplets on various solid substrates were obtained with the HMF. Contact angles were measured from these recorded images.

B. *Contact Angle Changes with Temperature and Magnetic-Flux Density*

Wetting behaviors of Al/AlN and Al/SiO_2 systems at different temperatures without and with HMF were explored, and the relationship of the contact angle and temperature is shown in Figure 2. The contact angle decreases with an increase in temperature at a 0 T magnetic field, which agrees with previous research, and contact angles that were measured without HMF were also comparable to the reported values for the same wetting systems.[36–38] Also, for 6 T HMF, the contact angles decrease with an increase in temperature. Contact angles maintained a 30 deg reduction compared with 0 T at different wetting temperatures when the magnetic-flux density was 6 T. For Al/AlN and Al/SiO_2, whether HMF exists or not, the contact angle only had a 2 to 3 deg decrease with a 30 °C increase in wetting temperature. Therefore, better wettability results from the application of HMFs rather than from an increase in temperature.

The effects of magnetic-flux density on the wetting behaviors of the Al/AlN and Al/SiO_2 systems were

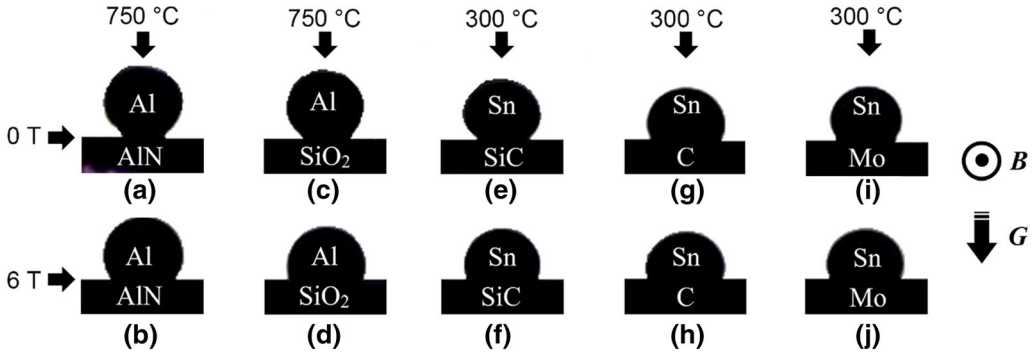

Fig. 1—Lateral images of molten metals spreading on different substrates. (*a*), (*c*) 750 °C, 0 T. (*b*), (*d*) 750 °C, 6 T. (*e*), (*g*), (*i*) 300 °C, 0 T. (*f*), (*h*), (*j*) 300 °C, 6 T.

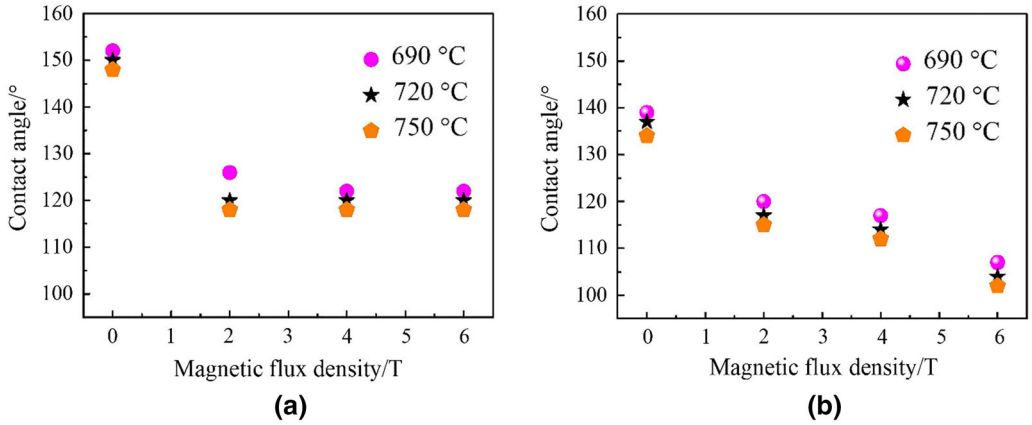

Fig. 2—Magnetic-flux-density dependence of the contact angles. (*a*) Al/AlN. (*b*) Al/SiO_2.

studied. Figure 2 shows variations of contact angles that result from a changing magnetic-flux density. Under the action of HMF, contact angles decreased, and the wettabilities of the Al/AlN and Al/SiO_2 systems were improved. The contact angle of Al/SiO_2 was smaller than that of Al/AlN under the same conditions. For Al/AlN, the increase in magnetic-flux density had no visible effect on the change in contact angle. For Al/SiO_2, a larger magnetic-flux density resulted in a smaller contact angle. The contact angles decrease with an increase in wetting temperature for different magnetic flux densities for Al/AlN and Al/SiO_2. In contrast, an increase in temperature for a specific magnetic-flux density is more effective than the effect of an increase in magnetic-flux density at a specific temperature for Al/AlN. This illustrates that the wettability of molten Al on the SiO_2 substrate is better than that on the AlN substrate.

The wetting behaviors of molten Sn with different substrates were investigated further. Without the effect of HMF, the contact angle of Sn/SiC decreased with an increase in temperature as shown in Figure 3(a). Under the action of HMF, contact angles showed a significant decreasing trend compared with the condition without HMF. At the same temperature, the contact angle measured in a 2 and 4 T high magnetic field has no obvious change. However, an increase in magnetic-flux density to 6 T resulted in a steep decrease in contact angle.

For Sn/C, as shown in Figure 3(b), without HMF, the contact angle decreased with an increase in temperature, whereas, the contact angle increased at a higher temperature in HMFs. The contact angle decreased with the effect of HMF. Otherwise, the contact angle measured at 4 T was larger than that measured at 2 and 6 T. The same change in wetting behavior resulted for Sn/Mo as shown in Figure 3(c). The effect of HMF on improving the wettability of Sn/Mo is more apparent than for Sn/C. Comparing the results presented in Figure 3, HMF has a beneficial effect on improving the wetting transition of molten Sn on different substrates by applying divergent magnetic flux densities. Furthermore, the effect of temperature on the Sn/SiC system is opposite to that in the Sn/C and Sn/Mo systems owing to the application of HMF. However, the contribution of the substrate in wetting process conducted in HMFs is not clear at present, and it will be investigated in further work.

The contact angles measured for different magnetic flux densities for Al/AlN, Al/SiO_2, Sn/SiC, Sn/C, and Sn/Mo at different wetting temperatures are summarized and given in Tables III, IV, V, VI, and VII, respectively. Compared with the published data in

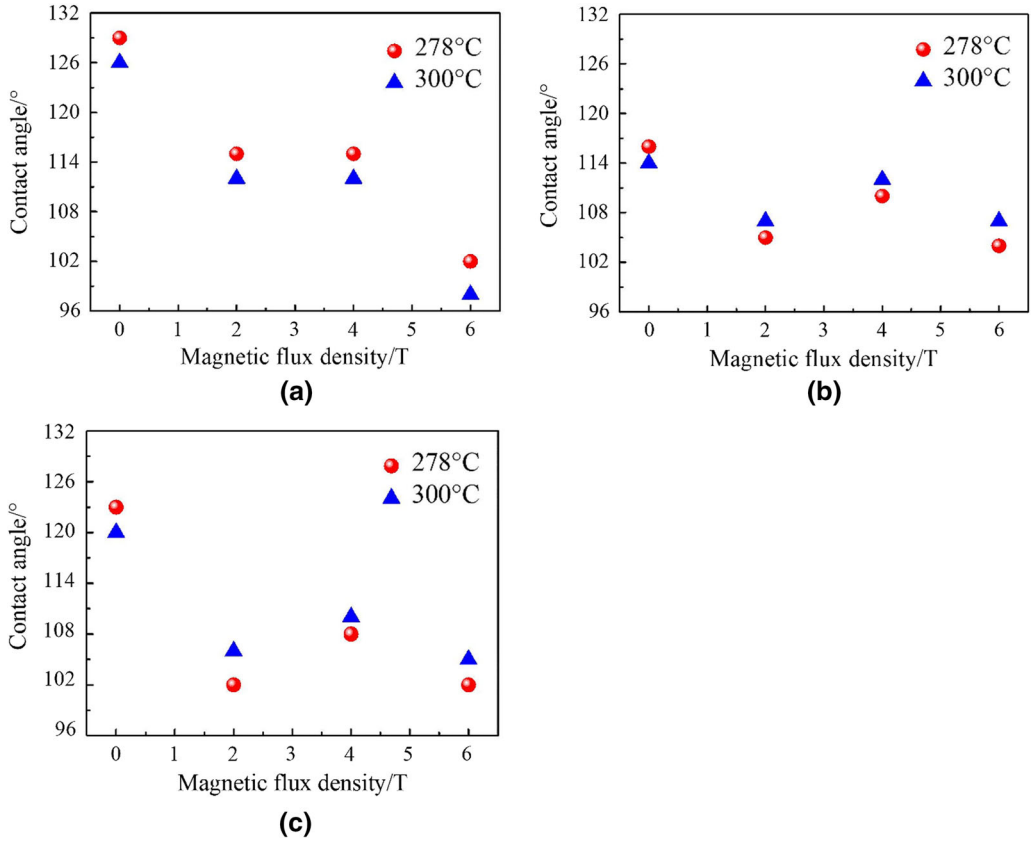

Fig. 3—Variations in contact angles with magnetic-flux density for molten Sn on different substrates at various temperatures. (*a*) Sn/SiC. (*b*) Sn/C. (*c*) Sn/Mo.

Table III. Contact Angles for Al/AlN

Temperature (°C)	690				720				750			
Magnetic-Flux Density (T)	0	2	4	6	0	2	4	6	0	2	4	6
Contact Angle (Deg)	152	126	122	122	150	120	120	120	148	118	118	118

Table IV. Contact Angles for Al/SiO_2

Temperature (°C)	690				720				750			
Magnetic-Flux Density (T)	0	2	4	6	0	2	4	6	0	2	4	6
Contact Angle (Deg)	139	120	117	107	137	117	114	104	134	115	112	102

Table V. Contact Angles for Sn/SiC

Temperature (°C)	278				300			
Magnetic-Flux Density (T)	0	2	4	6	0	2	4	6
Contact Angle (Deg)	129	115	115	102	126	112	112	98

earlier research, the contact angles measured without HMF are comparable,[39] which validates the current experimental facility and methodology. Thus, the experimental contact angles measured with or without HMFs for the Al/AlN, Al/SiO_2, Sn/SiC, Sn/C, and Sn/Mo systems are credible.

Table VI. Contact Angles for Sn/C

Temperature (°C)	278				300			
Magnetic-Flux Density (T)	0	2	4	6	0	2	4	6
Contact Angle (Deg)	116	105	110	104	114	107	112	107

Table VII. Contact Angles for Sn/Mo

Temperature (°C)	278				300			
Magnetic-Flux Density (T)	0	2	4	6	0	2	4	6
Contact Angle (Deg)	123	102	108	102	120	106	110	105

C. *Interface Characterization*

Wetting of AlN by molten Al is very complex, and divergent viewpoints exist. Some researchers propose that molten Al that spreads on the AlN substrate is reactive[38]; however, many other reports support that the Al/AlN wetting system is unreactive.[40] Solidified Al droplets adhered to the AlN substrate (Figures 4(a) and (b)) after wetting, and this phenomenon coincides with the characteristic of reactive wetting. Previous study has indicated that oxygen contaminants exist at the substrate-droplet interface and the decrease of oxygen content could lead to a better wetting status.[37] The morphology of the Al/AlN interface was tested by scanning electron microscopy (SEM), and the Al/AlN interface was approximately flat as shown in Figures 4(c) and (d). Without HMF, the element distribution tested from the surface to the inner of AlN substrate was tested by EDS line analysis, and the result is presented in Figure 4(e). For a 2 T HMF, EDS line-scan analysis across Al/AlN interface as shown in Figure 4(d) was carried out, and the result is shown in Figure 4(f). A comparison of the element distribution results shows that the oxygen content in the AlN substrate decreased with the effect of a 2 T HMF. An EDS line-scan analysis across the Al/AlN interface for 4 T and 6 T HMFs was tested as shown in Figures 4(g) and (h), respectively. The oxygen content in the AlN substrate that was used at different HMFs was lower than that measured in the AlN substrate without the effect of HMF. The oxygen contents in different AlN substrates for the HMFs that were studied were almost equal. Thus, the wetting-behavior change without and with the effect of HMFs can be attributed to the oxygen content change in the AlN substrate.

The wetting of SiO_2 by molten Al tends to belong to reactive wetting,[41] and this standpoint is confirmed here too. With or without HMF, a remarkable reaction layer exists at the Al/SiO_2 interface as the sample macrographs show in Figures 5(a) and (b). The hierarchical structures in the SiO_2 substrate are visible in the SEM images in Figures 5(c) and (d), and the reaction layer is located at the middle between the solidified Al droplet and SiO_2 substrate. The EDS line-scan analyses for the Al/reaction layer and the Al/reaction layer/SiO_2 substrate are shown in Figures 5(e) and (f). The element content nearly keeps constant from the Al/reaction layer interface to the reaction layer/SiO_2 substrate interface. Compared with the results from the 0 T HMF, there is a decrease in oxygen content in the reaction layer for a 2 T HMF. The EDS line-scan analyses across the reaction layer/SiO_2 interface at 4 T and the Al/reaction layer interface at 6 T are shown in Figures 5(g) and (h). The average oxygen contents in the reaction layer in the HMFs with a 4 T and 6 T magnetic-flux density are lower than those obtained from a 0 T HMF. The difference in oxygen content in the reaction layer for different magnetic-flux-density magnetic fields is not obvious. The oxygen content in the reaction layer affects the wetting behavior of the Al/SiO_2 system.[36] Thus, it can be deduced that the element distribution change in the reaction layer can lead to wetting-behavior changes of the Al/SiO_2 system that is regulated by HMF.

Figure 6 shows the Sn/C, Sn/SiC, and Sn/Mo sample morphologies after the wetting experiments. Solidified Sn droplets can separate themselves from all substrates with wetting for 0 T and 6 T HMF. The wetting counterparts of Sn/C, Sn/SiC, and Sn/Mo were unreactive in this work. Therefore, the effect of these factors with regards to the reactive wetting systems was not considered.

IV. DISCUSSION

The effect of gravity is an attractive discussion point for the elaboration of the wetting behavior; however, it is insufficient to affect wetting behavior if the liquid droplets are sufficiently small.[42,43] The qualities and dimensions of pure Al and Sn were selected according to prior research.[44] Except for the introduction of a magnetic field, there was no distinction between wetting for the same wetting raw materials of molten Al or Sn and substrate to conduct wetting experiments with and without HMF. Therefore, the effect of gravity during wetting can be excluded.

Samples of pure metal and substrate were placed in the center of the superconducting magnet during wetting. Another peculiar functional effect of HMF in material processing is the magnetic force, which is given as $F = V(1/\mu_0)\chi B(dB/dz)$, where V, μ_0, χ, B, and dB/dz are the volume, vacuum permeability, mass magnetic susceptibility per unit volume, magnetic-flux density, and magnetic field gradient, respectively.[45] Compared with the condition along the magnetic-field direction,

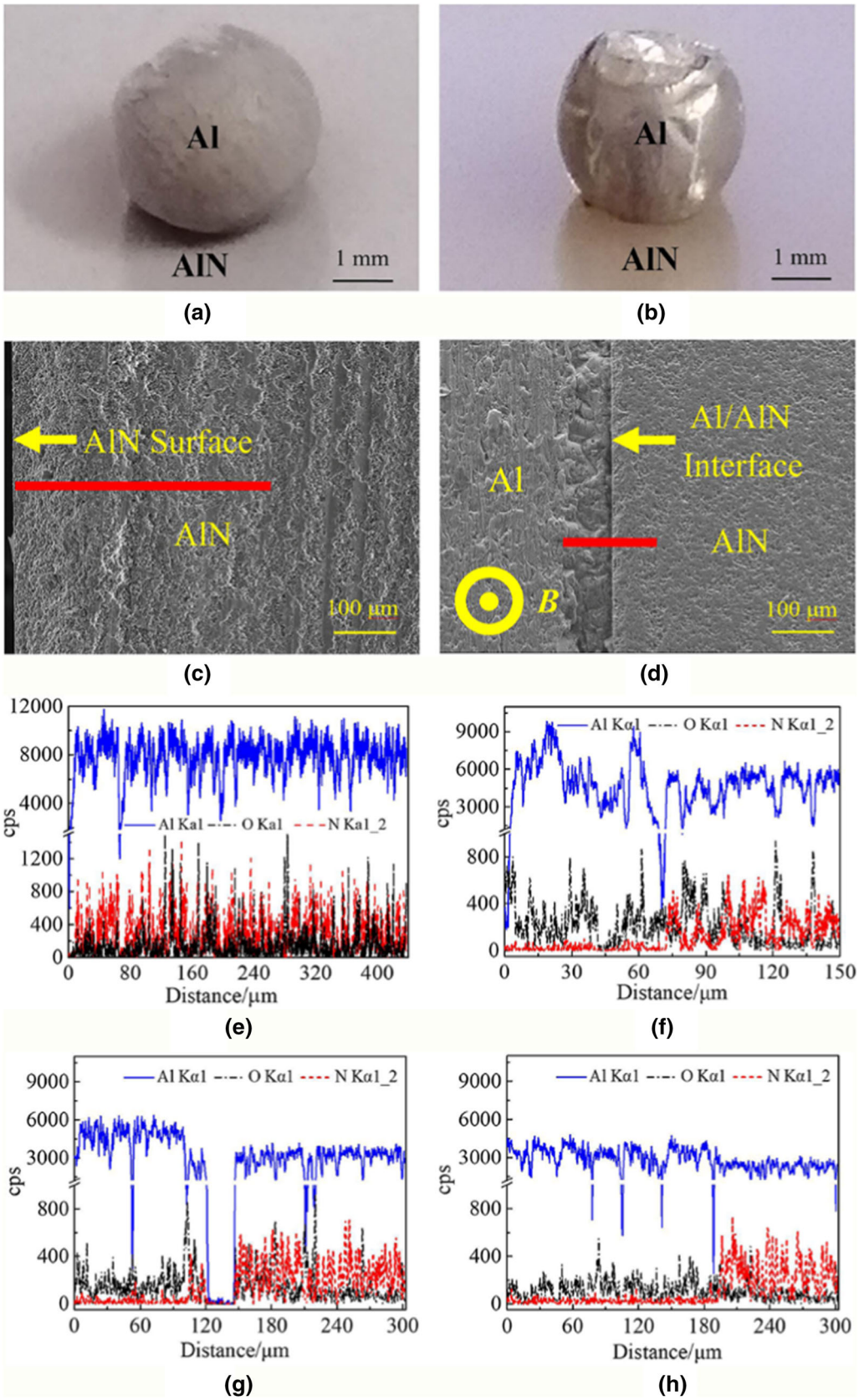

Fig. 4—Images of Al/AlN system after wetting experiments. (*a*) Macro image, 0 T. (*b*) Macro image, 2 T. (*c*) SEM image of the AlN substrate, 0 T. (*d*) SEM image of the Al/AlN interface, 2 T. (*e*) EDS line-scan analysis of the AlN substrate, 0 T. (*f*) EDS line-scan analysis across the Al/AlN interface, 2 T. (*g*) EDS line-scan analysis across the Al/AlN interface, 4 T. (*h*) EDS line-scan analysis across the Al/AlN interface, 6 T.

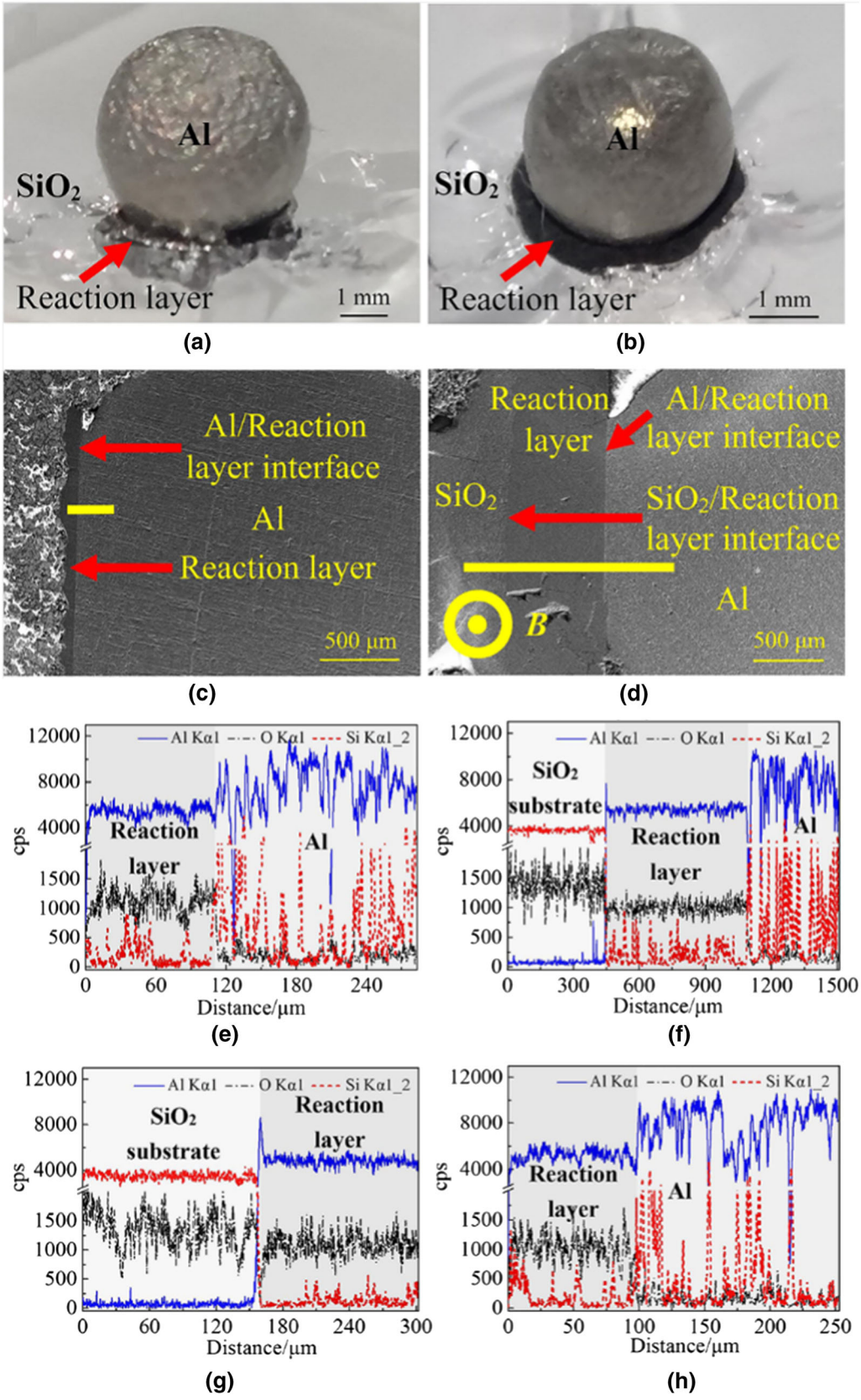

Fig. 5—Al/SiO_2 system after wetting experiments. (*a*) Macro image, 0 T. (*b*) Macro image, 2 T. (*c*) SEM image of the Al/reaction layer interface, 0 T. (*d*) SEM image of the Al/reaction layer/SiO_2 interface, 2 T. (*e*) EDS line-scan analysis across the Al/reaction layer interface, 0 T. (*f*) EDS line-scan analysis across the Al/reaction layer/SiO_2 interface, 2 T. (*g*) EDS line-scan analysis across the reaction layer/SiO_2 interface, 4 T. (*h*) EDS line-scan analysis across the Al/reaction layer interface, 6 T.

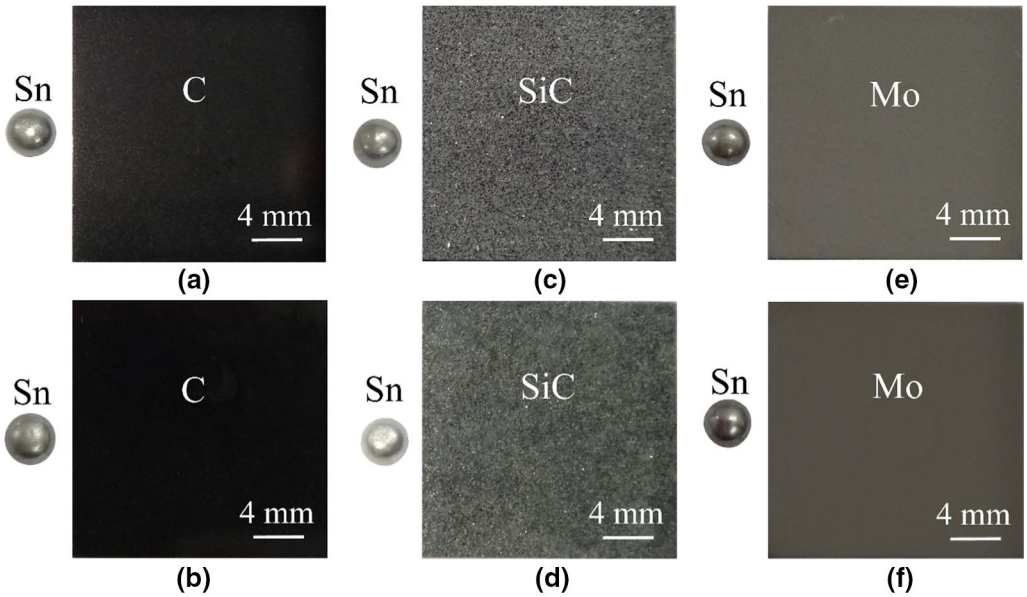

Fig. 6—Overview perspective morphologies after wetting experiments. (*a*) Sn/C, 0 T. (*b*) Sn/C, 6 T. (*c*) Sn/SiC, 0 T. (*d*) Sn/SiC, 6 T. (*e*) Sn/Mo, 0 T. (*f*) Sn/Mo, 6 T.

the magnetic-flux density and magnetic field gradient in the radial direction of the magnet are smaller and the effect of the magnetic force in the radial direction is negligible.

The distributions of magnetic-flux density and magnetic field gradient along the axial direction of the superconducting magnet are shown in Figure 7. The maximum magnetic-flux density, namely 6 T, is stable in a 4-mm-long range (labeled d_1), and pure metal and substrate were in this experimental range. Even if the spreading distance of the molten metal exceeds the range of d_1 and can reach d_2, which never exists in wetting experiments, the magnetic-flux density decreases to maintain a value of 5.998 T. Therefore, the magnetic-flux density of 5.998 T that considers the effect of the magnetic force is sufficient. The product of the magnetic-flux density and its gradient is 4.087 (T^2/m) in a 6 T HMF. The magnetic susceptibility of molten Sn was a linear function of temperature and was 0.0396×10^{-6} at its melting point.[30] The magnetic force is 0 N on the condition that molten Sn and substrate are at the magnet center. If not, the upper value of the magnetic force is 2.73×10^{-9} N. The density of molten Sn decreases linearly with an increase in temperature, and the density of molten Sn at its melting point is ~ 6.95 g/cm^3.[46] Thus, the gravity of molten Sn is ~ 1.47×10^{-3} N, which is larger than the magnetic force. The same analysis can be used for molten Al, and the magnetic susceptibility of molten Al at 700 °C is ~ 1.2×10^{-6}[47] and the density of molten Al at 700 °C is ~ 2.38 g/cm^3.[48] Hence, for molten Al, the magnetic force is 5.17×10^{-10} N and the gravity is 5.72×10^{-4} N, respectively. Based on the analysis, the influence of magnetic force in wetting transitions of molten Al and Sn with different substrates under HMFs can be neglected.

Wetting behavior is affected by temperature.[49] Conventionally, the contact angle will decrease to a smaller

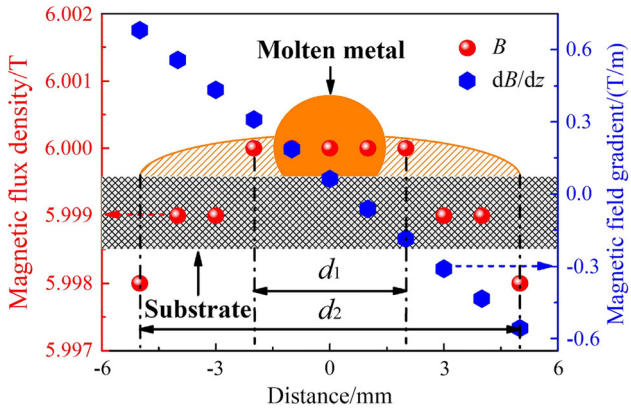

Fig. 7—Distribution of the symmetrical magnetic-flux density and magnetic field gradient in the axial direction of superconducting magnet.

value, and thus the wetting will improve because of the higher wetting temperature.[50] This change is an anastomosing description for Al/AlN, Al/SiO_2, and Sn/SiC counterparts as shown in Figures 2 and 3(a), respectively, with and without HMFs, and the Sn/C and Sn/Mo counterparts exhibited in Figures 3(b) and (c), respectively, without HMF. However, the contact angle increases with an increase of temperature for Sn/C and Sn/Mo with the influence of HMF. Therefore, HMF affects the wetting behaviors of SiC, C, and Mo substrates wetted by molten Sn and changes the effect of temperature. For the same kind of molten metal, the contact angles measured on different kinds of substrates are diverse at the same wetting temperature and magnetic flux density. This illustrates that the wetting transition is also influenced by substrate type. Furthermore, for reactive wetting, the wetting-behavior change regulated by HMFs results from the element content change in the substrate or reaction layer.

The contact angle initially decreases, then increases and decreases again with the increase of the magnetic-flux density for the Sn/C and Sn/Mo systems. For the Sn/SiC, HMF does not affect the wetting behavior apparently until the magnetic-flux density increases to 6 T. These results show that no linear relationship exists between the magnetic-flux density and contact angle.

Viscosity is sensitive to temperature, and previous research has confirmed that the change of the viscosity of molten metal with temperature is not monotonous, and a mutational viscosity exists in a certain temperature zone. The sudden change of viscosity of molten metal reflects the change of melt structure.[51] As a result, the surface energy is bound to change. Except for the temperature, the viscosity can be regulated by a magnetic field.[52] HMF controls melt flow,[53] and the melt flow status in a magnetic field affects the melt viscosity.[54,55] Voinov[56] indicated that the change of contact angle is dependent mainly on viscous dissipation during wetting. In addition, the effective viscosity of molten melt can be affected by the Lorentz force.[57] The combined action of temperature and HMF on the viscosity of molten Al and Sn may be the overriding factor that leads to the results in this work. Additionally, Eustathopoulos *et al.* revealed that the surface tension of pure aluminum decreased with the increase of temperature; however, there was no significant variation of the surface tension with time in the research on the surface tension of liquid aluminum.[58] Bainbridge and Taylor systematically measured the surface tension of molten metal, and they found that surface tension was subjected to the effect of substrate type.[59] Moreover, previous studies have validated that HMF can regulate surface tension[60] and magnetic energy.[61] In view of this, the wetting transition of molten metal on the solid substrate may be changed under the combined effect of the temperature and high magnetic field on surface tension and magnetic energy in the wetting process.

The outline deformation can directly reflect the change of contact angle in wetting transition. There are some small deformations that are not obvious for the outline of the molten metal as shown in Figure 1. Previous study has testified that convection in metallic melts could be suppressed by the Lorentz force in a static magnetic field.[62] Therefore, the Lorentz force will give rise to the small deformation of molten metal in the wetting process at different magnetic flux densities.

The high magnetic field effects on the wetting transition in the molten metal and solid substrate system have been linked to the element migration, viscosity, surface tension, magnetic energy, and small deformation. However, the information provided by the present experiment is insufficient to completely reveal the mechanism of the observed magnetic field effects, and further systematic work is required.

V. CONCLUSIONS

In this work, the wetting transition of molten metals on solid substrates in HMFs were investigated using the sessile drop method. With HMFs, the contact angles of Al/AlN, Al/SiO_2, Sn/SiC, Sn/C, and Sn/Mo systems all decreased, indicating a noticeable improvement of the wettability of these systems. The contact angle remained almost unchanged for the Al/AlN, whereas it decreased for Al/SiO_2 and Sn/SiC and increased first and then decreased for Sn/C and Sn/Mo, with increasing magnetic flux density. Without HMF, the contact angle for all systems decreased with increasing temperature. However, with HMFs, the contact angle decreased for Al/AlN, Al/SiO_2, and Sn/SiC, but increased for Sn/C and Sn/Mo, with increasing temperature. For reactive wetting systems, namely Al/AlN and Al/SiO_2, the influence of HMF on element distribution in the molten metal and substrate interface gave rise to the wetting transition change. For non-reactive wetting systems, *i.e.*, Sn/SiC, Sn/C, and Sn/Mo, the wetting transition change probably results from the physical property change of molten metals induced by HMFs. This method of regulating the wetting transition by HMFs is feasible and meaningful.

ACKNOWLEDGMENTS

The authors are grateful for the financial support from the National Natural Science Foundation of China (Grant Nos. 51774086, 51574073, 51425401, and 51690161), Fundamental Research Funds for the Central Universities (Grant Nos. N180915002, N170902002, and N170908001), and Liaoning Innovative Research Team in University, China (Grant No. LT2017011).

REFERENCES

1. A. Wat, J.I. Lee, C.W. Ryu, B. Gludovatz, J. Kim, A.P. Tomsia, T. Ishikawa, J. Schmitz, A. Meyer, M. Alfreider, D. Kiener, E.S. Park, and R.O. Ritchie: *Nat. Commun.*, 2019, vol. 10, art. no. 961.
2. J.R. Kang, X.G. Song, S.P. Hu, D. Liu, W.J. Guo, W. Fu, and J. Cao: *Metall. Mater. Trans. A*, 2017, vol. 48A, pp. 5870–78.
3. K. Zeng and K.N. Tu: *Mater. Sci. Eng. R*, 2002, vol. 38, pp. 55–105.
4. J. Rafiee, X. Mi, H. Gullapalli, A.V. Thomas, F. Yavari, Y.F. Shi, P.M. Ajayan, and N.A. Koratkar: *Nat. Mater.*, 2012, vol. 11, pp. 217–22.
5. Q. Wang, B. Xu, Q. Hao, D. Wang, H. Liu, and L. Jiang: *Nat. Commun.*, 2019, vol. 10, art. no. 1212.
6. V. Bergeron, D. Bonn, J.Y. Martin, and L. Vovelle: *Nature*, 2000, vol. 405, pp. 772–75.
7. N.S. Dhillon, J. Buongiorno, and K.K. Varanasi: *Nat. Commun.*, 2015, vol. 6, art. no. 8247.
8. A.J. Klinter, C.A. Leon-Patiño, and R.A.L. Drew: *Acta Mater.*, 2010, vol. 58, pp. 1350–60.
9. G. Kumar and K.N. Prabhu: *Adv. Colloid Interfac.*, 2007, vol. 133, pp. 61–89.
10. N. Ray, L. Froyen, K. Vanmeensel, and J. Vleugels: *Acta Mater.*, 2018, vol. 144, pp. 459–69.
11. N. Eustathopoulos: *Acta Mater.*, 1998, vol. 46, pp. 2319–27.
12. P. Nautiyal, A. Gupta, S. Seal, B. Boesl, and A. Agarwal: *Acta Mater.*, 2017, vol. 126, pp. 124–31.
13. F. Wang, A. Reiter, M. Kellner, J. Brillo, M. Selzer, and B. Nestler: *Acta Mater.*, 2018, vol. 146, pp. 106–18.
14. H. Fujii, S. Izutani, T. Matsumoto, S. Kiguchi, and K. Nogi: *Mater. Sci. Eng. A*, 2006, vol. 417, pp. 99–103.

15. J.-G. Li and J. Gao: *Mater. Lett.*, 2006, vol. 60, pp. 1323–26.
16. C.H. Jang, S.I. Paik, Y.W. Kim, and N.-E. Lee: *Appl. Phys. Lett.*, 2007, vol. 90, art. no. 091915.
17. M. Lei, J.C. Feng, X.Y. Tian, J.M. Shi, and L.X. Zhang: *Vacuum*, 2017, vol. 138, pp. 22–29.
18. Q. Wang, M. Dong, J. Sun, T. Liu, and Y. Yuan: *Acta Metall. Sin.*, 2018, vol. 54, pp. 742–56.
19. Y. Miyazawa, S. Morita, and H. Sekiwa: *J. Cryst. Growth*, 1996, vol. 166, pp. 286–90.
20. T.P. Hou and K.M. Wu: *Scripta Mater.*, 2012, vol. 67, pp. 609–12.
21. D. Du, Y. Fautrelle, Z. Ren, R. Moreau, and X. Li: *Acta Mater.*, 2016, vol. 121, pp. 240–56.
22. Q. Wang, D.-G. Li, K. Wang, Z.-Y. Wang, and J.-C. He: *Scripta Mater.*, 2007, vol. 56, pp. 485–88.
23. Y. Ikezoe, N. Hirota, J. Nakagawa, and K. Kitazawa: *Nature*, 1998, vol. 393, pp. 749–50.
24. Y. Zhang, N. Gey, C. He, X. Zhao, L. Zuo, and C. Esling: *Acta Mater.*, 2004, vol. 52, pp. 3467–74.
25. D. Vriami, E. Beaugnon, J.-P. Erauw, J. Vleugels, and O. Van der Biest: *J. Eur. Ceram. Soc.*, 2015, vol. 35, pp. 3959–67.
26. Y.-M. Liu, R.-Q. Chen, Z.-Q. Wu, J. Zhu, J.-Y. Shi, H.-M. Lu, P. Shang, and D.-C. Yin: *Rev. Sci. Instrum.*, 2016, vol. 87, art. no. 095107.
27. C. Li, Y. Cao, R. Guo, S. He, W. Xuan, X. Li, Y. Zhong, and Z. Ren: *Rev. Sci. Instrum.*, 2017, vol. 88, art. no. 115110.
28. Y. Xiao, T. Liu, Z. Lu, S. Yuan, G. Li, S. Dong, and Q. Wang: *Rev. Sci. Instrum.*, 2019, vol. 90, art. no. 063902.
29. G.E. Totten and D.S. MacKenzie: *Handbook of Aluminum*, Marcel Dekker Inc, New York, 2003, pp. 47–49.
30. H.R. Leo and F.J. Simmons: *J. Magn. Magn. Mater.*, 1988, vol. 74, pp. 87–90.
31. G.R. Prin, T. Baffie, M. Jeymond, and N. Eustathopoulos: *Mater. Sci. Eng. A*, 2001, vol. 298, pp. 34–43.
32. H. Zhu, K. Dong, J. Huang, J. Li, G. Wang, and Z. Xie: *Mater. Chem. Phys.*, 2014, vol. 145, pp. 334–41.
33. G.W. Liu, M.L. Muolo, F. Valenza, and A. Passerone: *Ceram. Int.*, 2010, vol. 36, pp. 1177–88.
34. Z. Weltsch, A. Lovas, J. Takács, Á. Cziráki, A. Toth, and G. Kaptay: *Appl. Surf. Sci.*, 2013, vol. 268, pp. 52–60.
35. M. Wu, L. Chang, L. Zhang, X. He, and X. Qu: *Surf. Coat. Tech.*, 2016, vol. 287, pp. 145–52.
36. X.B. Zhou and J.Th.M. De Hosson: *Acta Mater.*, 1996, vol. 44, pp. 421–26.
37. H.-N. Ho and S.-T. Wu: *Mater. Sci. Eng. A*, 1998, vol. 248, pp. 120–24.
38. M. Kida, M. Bahraini, J.M. Molina, L. Weber, and A. Mortensen: *Mater. Sci. Eng. A*, 2008, vol. 495, pp. 197–202.
39. S.A. Sánchez, J. Narciso, E. Louis, F. Rodríguez-Reinoso, E. Saiz, and A. Tomsia: *Mat. Sci. Eng. A*, 2008, vol. 495, pp. 187–91.
40. N. Eustathopoulos, M.G. Nicholas, and B. Drevet: *Wettability at High Temperatures*, Elsevier Science Ltd., Oxford, 1999, pp. 283–91.
41. N. Eustathopoulos, D. Chatain, and L. Coudurier: *Mat. Sci. Eng. A*, 1991, vol. 135, pp. 83–88.
42. C.W. Extrand: *J. Colloid Interf. Sci.*, 1993, vol. 157, pp. 72–76.
43. Š. Šikalo, M. Marengo, C. Tropea, and E.N. Ganić: *Exp. Therm. Fluid Sci.*, 2002, vol. 25, pp. 503–10.
44. P. Shen, H. Fujii, and K. Nogi: *Acta Mater.*, 2006, vol. 54, pp. 1559–69.
45. M. Dong, T. Liu, J. Liao, Y.-B. Xiao, Y. Yuan, and Q. Wang: *J. Alloy. Compd.*, 2016, vol. 689, pp. 1020–27.
46. I. Kaban, S. Gruner, and W. Hoyer: *J. Non-Cryst. Solids*, 2007, vol. 353, pp. 3717–21.
47. P. Terzieff and R. Lück: *J. Alloy. Compd.*, 2003, vol. 360, pp. 205–09.
48. V. Sidorov, I. Polovov, B. Rusanov, N. Katkov, V. Mikhailov, P. Popel, K. Maksimtsev, A. Mukhamadeev, and G. Patronov: *J. Alloy. Compd.*, 2019, vol. 787, pp. 1345–48.
49. Y. Zhao, Y. Wang, Y. Zhou, and P. Shen: *Scripta Mater.*, 2011, vol. 64, pp. 229–32.
50. H. Fujii and S. Izutani: *J. Mater. Sci.*, 2012, vol. 47, pp. 8387–94.
51. C. Sun, H. Geng, Z. Yang, J. Zhang, and R. Wang: *Mater. Charact.*, 2005, vol. 55, pp. 383–87.
52. T. Mao, X. Bian, S. Morioka, Y. Wu, X. Li, and X. Lv: *Phys. Lett. A*, 2007, vol. 366, pp. 155–59.
53. H. Yasuda, I. Ohnaka, O. Kawakami, K. Ueno, and K. Kishio: *ISIJ Int.*, 2003, vol. 43, pp. 942–49.
54. W. Chester: *J. Fluid Mech.*, 1961, vol. 10, pp. 459–65.
55. W. Chester and D.W. Moore: *J. Fluid Mech.*, 1961, vol. 10, pp. 466–72.
56. O.V. Voinov: *Fluid Dyn.*, 1976, vol. 11, pp. 714–21.
57. Q. Wang, C.-J. Wang, T. Liu, K. Wang, and J.-C. He: *J. Mater. Sci.*, 2007, vol. 42, pp. 10000–06.
58. J.M. Molina, R. Voytovych, E. Louis, and N. Eustathopoulos: *Int. J. Adhes. Adhes.*, 2007, vol. 27, pp. 394–401.
59. I.F. Bainbridge and J.A. Taylor: *Metall. Mater. Trans. A*, 2013, vol. 44A, pp. 3901–09.
60. Y. Fujimura and M. Iino: *J. Appl. Phys.*, 2008, vol. 103, art. no. 124903.
61. C. Li, L. Chen, and Z. Ren: *J. Mol. Liq.*, 2013, vol. 181, pp. 51–54.
62. H. Yasuda, I. Ohnaka, Y. Ninomiya, R. Ishii, S. Fujita, and K. Kishio: *J. Cryst. Growth*, 2004, vol. 260, pp. 475–85.